Available online at www.sciencedirect.com
SCIENCE DIRECT
Polymer 45 (2004) 7129–7136
polymer
www.elsevier.com/locate/polymer

Preparation and magnetometric characterization of iron oxide-containing alginate/poly(vinyl alcohol) networks

Yoshiyuki Nishio[a,*], Akiko Yamada[b], Kana Ezaki[b], Yoshiharu Miyashita[b], Hidemitsu Furukawa[b], Kazuyuki Horie[b]

[a]*Division of Forest and Biomaterials Science, Graduate School of Agriculture, Kyoto University, Kyoto 606-8502, Japan*
[b]*Department of Organic and Polymer Materials Chemistry, Tokyo University of Agriculture and Technology, Koganei, Tokyo 184-8588, Japan*

Received 18 May 2004; received in revised form 11 August 2004; accepted 23 August 2004

Abstract

Alginate-based magnetic gels were prepared in a sequence of procedures for in situ synthesis of iron oxides: crosslinking of alginate in ferrous salt aqueous solution, immersion of the resulting gels into alkaline-earth metallic hydroxide solution, and treatment of the partially cation-exchanged gels with hydrogen peroxide. Magnetometry measurements revealed that the lyophilized gels showed superparamagnetism or ferromagnetism at room temperature, depending on the sort of the metallic cation employed in the alkali treatment. An interpenetrating network (IPN) type of alginate/poly(vinyl alcohol) (Alg/PVA) gels containing iron oxides was also designed and fabricated from mixed polymer solutions by a modified preparation method; the gelation and alkali treatment were carried out with the aid of a metallic borate. Viscoelasticity of the magnetic IPN composites in the gelatinous state was controllable by changing the mixing ratio of the compatible carbohydrate/viny polymer pair. Magnetization versus magnetic field curves were constructed at different temperatures for the IPNs freeze-dried. Their magnetic character was variable according to alterations of the Alg/PVA composition, alkaline reagent adopted, and measurement temperature.

Keywords: Alginate/poly(vinyl alcohol) IPN; Iron oxide; Magnetic composites

1. Introduction

Naturally occurring polysaccharides have been reevaluated as a mass of renewable resources in recent years. They are environmentally friendly substances and also possess a high potential to be newly developed for industrial and medical applications in themselves or in combination with supplementary organic or inorganic compounds. As a functional development toward advanced materials, the designing of magnetic composites based on cellulose and related polysaccharides has attracted considerable attention in the past decade [1–9], in relation to the possibilities of specialty uses as information-transferring or storing media, fabrics of electromagnetic shielding, new filtration and separation systems, and so forth. A major technique for the compositions is an in situ synthesis [10] of iron oxide nanoparticles in fibrillar suspensions or gels of polysaccharides, rather than physical loading of magnetic pigments into the polymer matrices. The standard of the chemical synthesis consists of three steps: (1) ferrous ion-absorption of original polymer materials following their swelling or gelation in a ferrous salt solution; (2) in situ precipitation of ferrous hydroxide by a mild alkaline treatment of the swollen polymers usually with aqueous sodium hydroxide; (3) oxidation of the ferrous hydroxide with an oxidizing agent. Among the works along this line, there were a few attempts made to prepare alginate-based magnetic composites in the form of spherical beads [5,8], possibly useful in biomedical and pharmaceutical fields, e.g., as a magnetic drug-delivery system [3].

Alginate is an electrolytic polysaccharide supplied in plenty from marine algae. The molecular structure is

* Corresponding author. Tel.: +81-75-753-6250; fax: +81-75-753-6300.
E-mail address: ynishio@kais.kyoto-u.ac.jp (Y. Nishio).

0032-3861/$ - see front matter © 2004 Elsevier Ltd. All rights reserved.
doi:10.1016/j.polymer.2004.08.047

composed of β-D-mannuronate (M) and α-L-guluronate (G) residues; however, they are arranged in a block-wise fashion, constructed not only of homo-polyuronate blocks (MM or GG) but also of alternating blocks (MG) [11,12]. An aqueous solution of alginate is readily transformed into a hydrogel on addition of metallic divalent cations such as Ca^{2+} [13,14], and the gelation behaviour has been investigated in various ways [15,16]. It has been generally accepted that crosslinks are formed by coordination of divalent metallic cations to the interchain cavities made up of GG blocks, resulting in development of a so-called 'egg-box' junction zone [14,17].

The crosslinked alginate gels are relatively rigid, but usually fragile; this may be a disadvantage particularly for a ferrous alginate gel in caustic alkaline atmosphere, which was just the situation employed for preparation of iron oxides therein [5,8]. The rigid and fragile nature of gelatinous alginates may also be unfavorable in processing into non-spherical forms such as films and filaments via the gel state. A method to overcome the drawback is blending the polysaccharide compatibly with a flexible vinyl polymer. As was shown in a previous work by the authors' group [18], fortunately, sodium alginate can form blend films compatible with poly(vinyl alcohol) (PVA), when cast from mixed polymer solutions in water. Furthermore, a post-treatment of the as-cast samples with a calcium tetraborate solution leads to the development of an interpenetrating polymer network (IPN) structure, via concurrence of the chelate complexing of alginate with calcium cation and a borate ion-aided crosslinking between PVA chains.

The present paper is mainly concerned with the preparation and magnetometric characterization of an IPN type of composites of Alg/PVA incorporated with iron oxide particles, which are precipitated chemically within the binary polymer networks. An insight is also provided into an effect of alkaline treatment conditions on the magnetic property of alginate-iron oxide composites prepared by the in situ synthesis method.

2. Experimental

2.1. Original materials

The alginate material used was a commercial product of sodium alginate (NaAlg), Duck Algin 350 (Lot No. 34590) purchased from Kibun Food Chemifa Co. (Japan). The molar ratio of M to G units was 1.02, which was determined by ^{13}C NMR spectroscopy, following the peak assignments given in a literature [19]. Poly(vinyl alcohol) (PVA) was supplied as PVA-HC by Kuraray Co.; the nominal degree of polymerization was 1750 and the saponification value was 99.9 mol%.

$FeSO_4$ or $FeCl_2$ was used to make ferrous alginate gels; the inorganic salts of Fe(II) were obtained in the heptahydrate and tetrahydrate forms, respectively, from Kanto Chemical Co., Inc. As a crosslinker for PVA and/or alginate, sodium tetraborate ($Na_2B_4O_7$) and calcium tetraborate (CaB_4O_7) were purchased from Kanto Chemical Co., Inc. and Soekawa Chemical Co. Ltd., respectively. The other chemicals used, $Ca(OH)_2$, $Sr(OH)_2$, $Ba(OH)_2$, and an aqueous H_2O_2 solution were all reagent grade.

2.2. Preparation of iron oxide-containing alginate samples

The following procedures except for an oxidizing step were carried out in an atmosphere of nitrogen. The distilled water used was degassed with N_2-bubbling, after standing under reduced pressure.

An aqueous solution of NaAlg was prepared at a concentration of 2.5 wt%. The desired amount (5.0 g) was poured into a Teflon tray and spread on a flat bottom. The tray containing the layered viscous polymer solution was carefully immersed in an appropriate quantity (~100 ml) of ferrous sulfate or chloride hydrate solution (0.025 M) as coagulant. After standing for 24 h at room temperature, the resulting gel was taken out of the coagulant bath and steeped in a large amount of distilled water which was exchanged for fresh aliquots several times. The thoroughly washed ferrous alginate gel (Fe-Alg), imparting a yellowish hue, was then steeped for 24 h in an aqueous alkaline solution (~100 ml, pH≈12.5) prepared with a 0.0135 M hydroxide of calcium, strontium, or barium; whereupon the gel turned deep-greenish. The alkaline water bath was heated to 65 °C and 1% hydrogen peroxide solution (~10 ml) was added there into dropwise over a period of ~15 min. The oxidized gel (o-Fe-Alg), colored reddish brown, was washed with distilled water and, as occasion demanded, air-dried or lyophilized.

Selected samples of gelatinous o-Fe-Algs were further oxidized in additional cycles involving the ferrous ion-absorption, alkali treatment, and oxidation with H_2O_2 described above.

2.3. Preparation of iron oxide-containing Alg/PVA IPNs

Aqueous solutions of NaAlg and PVA were prepared separately at concentrations of 2.5 and 13.2 wt%, respectively; the latter polymer material (powder) was dissolved in water at ~95 °C with continuous stirring. The two viscous solutions were mixed in the desired proportions at room temperature and then stirred overnight. The mixed solutions were optically clear and showed no separation into bilayers nor any precipitation, irrespective of the relative polymer composition ranging from 7/3 to 3/7 in Alg/PVA weight ratio.

IPN-type Alg/PVA gels containing iron oxide particles were prepared in a similar process as above, but the samples were made in a half scale and the step of gelation/Fe^{2+}-absorption and that of alkali treatment were modified adequately. First, each blend solution was gelatinized

moderately by applying a sodium or calcium tetraborate solution at a concentration of $<0.04\%$ in weight percent of salt to polymer. The application of $Na_2B_4O_7$ allows the PVA component to crosslink, while the treatment with CaB_4O_7 leads the generation of crosslinks in both polymer components; i.e., borate-aided crosslinks between PVA chains and chelate complexing of alginate chains with Ca^{2+}. The Alg/PVA samples thus pretreated were immersed in a ferrous sulfate solution (0.025 M), which resulted in a tighter network system (Fe-Alg/PVA) imparting a light-yellow color, due to incorporation of Fe^{2+} therein.

The alkali treatment of Fe-Alg/PVA's was carried out at $\sim$20 °C with a 0.0135 M aqueous solution of CaB_4O_7 (pH$\approx$9.2) and/or that of $Ca(OH)_2$ (pH$\approx$12.5), in different ways of steeping: (a) in a CaB_4O_7 bath for 24 h; (b) first in a CaB_4O_7 bath for 12 h and then in a $Ca(OH)_2$ bath for additional 12 h; (c) in an equimolar $CaB_4O_7/Ca(OH)_2$ bath for 24 h; (d) in a $Ca(OH)_2$ bath for 24 h.

The major samples (o-Fe-series) used for magnetometry are listed in Table 1, together with the crosslinking and alkali-treating regents employed for the preparation.

2.4. Measurements

The content of iron in the respective composites described above was determined by a reduction/oxidation titration method. Ferric ions were extracted from a weighed sample of each dried gel with a warmed HCl solution, then reduced to Fe^{2+} with the aid of tin(II) chloride. The ferrous ionic solution was titrated with potassium dichromate by using sodium diphenylamine-4-sulfonate as an indicator. In what follows, the iron content is denoted as a weight percent to the dried composite sample.

Magnetometry measurements were carried out on 3–6 mg samples (freeze-dried) with a superconducting quantum interference device (SQUID), MPMS-5 of Quantum Design Inc. The magnetic field (H) applied was usually varied as $0\rightarrow5\times10^4$ G$\rightarrow-10^3$ G$\rightarrow0$ at a constant temperature. For a given sample, data of the magnetization (M) were collected at 300 (or 298), 200, 100, and 20 K.

The viscoelastic property of Alg/PVA gels containing iron oxides was examined with a rheometric dynamic mechanical analyzer RSA II. Test specimens were prepared in a dimension of 5 mm diameter and 2.5–4 mm thick. The dynamic storage modulus E', loss modulus E'', and loss tangent tan δ were measured at 20 °C in a compression mode, the oscillatory frequency ranging from 0.159 to 15.9 Hz.

3. Results and discussion

3.1. Iron oxide-containing alginate samples

Visual inspection of the coloration of alginate gels, changing from yellowish ocher (Fe-Alg) to ruddy brown (o-Fe-Alg), indicated a successful incorporation of iron oxide particles (synthetic ferrites) into the polysaccharide matrix. As has been pointed out for other examples by similar preparation methods [5,6,8], however, less magnetic ferric oxyhydroxide (FeOOH) would be coexistent in the

Table 1
Preparation condition of iron oxide-incorporated Alg/PVA samples, and their iron content and responsiveness to a conventional magnet

Sample code	Alg/PVA composition	Pre-crosslinking agent	Reagent of alkali treatment	Fe content[a]/wt%	Response to magnet at RT
o-Fe-B1	0/10	$Na_2B_4O_7$	(a) CaB_4O_7	–	No
o-Fe-B2	5/5	CaB_4O_7	(a) CaB_4O_7	7.3	No
o-Fe-B3	5/5	$Na_2B_4O_7$	(a) CaB_4O_7	5.7	No
o-Fe-B4	7/3	$Na_2B_4O_7$	(a) CaB_4O_7	5.4	No
o-Fe-B5	10/0	$Na_2B_4O_7$	(a) CaB_4O_7	9.8	No
o-Fe-B6	5/5	$Na_2B_4O_7$	(d) $Ca(OH)_2$	11.2	Yes
o-Fe-B7	5/5	CaB_4O_7	(b) CaB_4O_7 and $Ca(OH)_2$, separated	6.3	Yes
o-Fe-B8	5/5	$Na_2B_4O_7$	(b) CaB_4O_7 and $Ca(OH)_2$, separated	4.0	Yes
o-Fe-B9	7/3	$Na_2B_4O_7$	(c) $CaB_4O_7/Ca(OH)_2$ mixture	7.4	Yes
o-Fe-B10	7/3	CaB_4O_7	(c) $CaB_4O_7/Ca(OH)_2$ mixture	7.0	Yes
o-Fe-B11	5/5	$Na_2B_4O_7$	(c) $CaB_4O_7/Ca(OH)_2$ mixture	5.6	Yes
o-Fe-B12	5/5	CaB_4O_7	(c) $CaB_4O_7/Ca(OH)_2$ mixture	7.0	Yes
o-Fe-Alg(Ca)	10/0	–	(d) $Ca(OH)_2$	11.7 (18.9)[b]	Yes
o-Fe-Alg(Sr)	10/0	–	$Sr(OH)_2$	10.1	Yes
o-Fe-Alg(Ba)	10/0	–	$Ba(OH)_2$	8.4	Yes

[a] Percentage to the respective dried samples.
[b] Data obtained after three cycles of the reaction for iron oxide synthesis.

composites, in addition to familiar magnetic ferric oxide (γ-Fe_2O_3) and ferrous ferric oxide (Fe_3O_4). The coloring behaviour was observed in common for any alginate samples subjected to the present in situ synthesis reaction, irrespective of the sort of the alkaline-earth metallic hydroxide used ($Ca(OH)_2$, $Sr(OH)_2$, or $Ba(OH)_2$) as well as that of the ferrous salt ($FeCl_2$ or $FeSO_4$). The oxidized gels of reddish-brown were responsive to a conventional bar magnet, evidently attracted by this. Iron contents of the o-Fe-Algs ranged roughly from 8 to 12 wt% in their dried state after one cycle of the reaction. In a control experiment with a trivalent Fe-salt such as $FeCl_3$ and $Fe_2(SO_4)_3$ in the first step of composite preparation, aqueous alginate was also gelatinized with accompanying absorption of Fe^{3+} ions, but no systematic change in color of the resulting gel (orange) was discernible in the subsequent steps. Deservedly, the final product was insensitive to the bar magnet.

The choice of sulfate or chloride as the ferrous salt to make Fe-Alg gels was not a factor affecting the magnetization property of o-Fe-Algs finally obtained. Concerning the hydroxyl compound in the alkali-treating step, however, the difference in the metallic cation gave rise to a distinction in magnetic character between the three series of o-Fe-Alg samples, when examined in a SQUID magnetometry at 300 K, as demonstrated below.

Alginates crosslinked with iron salts were, as such, all paramagnetic, i.e., the magnetization M increased proportionally with increasing applied field H, as exemplified in Fig. 1. The behaviour is ascribable to the paramagnetism of the iron ions incorporated, since the original sodium alginate and its acid form were essentially diamagnetic, giving quite a small negative value of magnetic susceptibility. On oxidizing ferrous alginates (Fe-Algs) via the treatment with $Ca(OH)_2$, the products provided a characteristic M versus H profile in which a steep rise of magnetization occurred around the origin ($H < 100$ G) and there appeared no coercive force or remanent magnetization. Fig. 1 illustrates the typical data for an o-Fe-Alg sample (coded as o-Fe-Alg(Ca) in Table 1). Then the magnetism of such a composite may be regarded as superparamagnetic, which is usually observed when the magnetic particles are dispersed in the matrix in a scale of less than a few tens of nanometers.

Fig. 2 displays magnetization curves obtained for other two alginate composites which were prepared by employing $Sr(OH)_2$ and $Ba(OH)_2$, respectively, in the step of alkali treatment. Differing from the superparamagnetic character of o-Fe-Alg(Ca), the two additional samples, coded as o-Fe-Alg(Sr) and o-Fe-Alg(Ba) in Table 1, are ferromagnetic substances in a wide sense, providing a hysteresis loop with definitely nonzero values of remanent magnetization (M_r) and coercive force (H_c). Also, the two data give a relatively large saturation magnetization (M_s) in comparison with the result for o-Fe-Alg(Ca). The difference in magnetism between the three alginate composites is summarized in Table 2. The M_s values compiled there were determined, for convenience, by regression of the respective magnetization data in a range of 0–1000 G in terms of the following classical Langevin function [20]:

$$M = M_s[\coth(\alpha) - \alpha^{-1}] \quad (1)$$

with $\alpha = \mu H/kT$, where μ is a magnetic moment per particle, k is the Boltzman constant, and T denotes absolute temperature.

In the alkali treatment of Fe-Alg gels, as an ideal case of the in situ reaction, ferrous hydroxide would precipitate to be confined within a nanoscale space, in close vicinity of the crosslinking points of the alginate network. This should accompany partial exchanging between Fe^{2+} and the alkaline-earth metallic ion employed, wherewith the latter divalent cation, in turn, participates in retention of the egg-box junctions in cooperation with carboxy anions. If the replacing cation is univalent, such as Na^+ and K^+, the crosslinking network is much loosened or destroyed, which was confirmed actually. Calcium cation, only a little larger

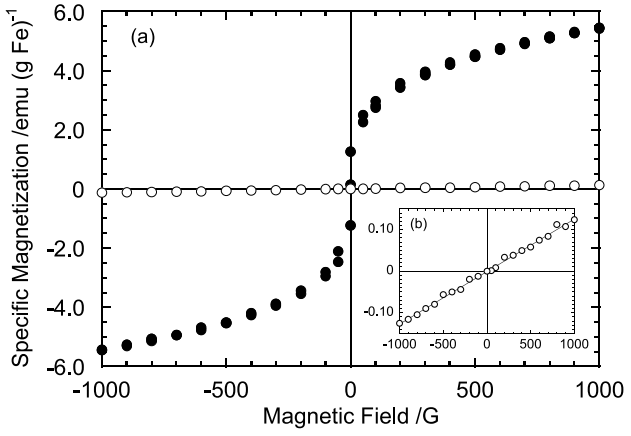

Fig. 1. Magnetization versus magnetic field plots for freeze-dried samples of Fe-Alg (as crosslinked with ferrous sulfate) and o-Fe-Alg(Ca), measured at 300 K: (○), data for Fe-Alg; (●), data for o-Fe-Alg(Ca). (b) shows the data for Fe-Alg on an enlarged scale.

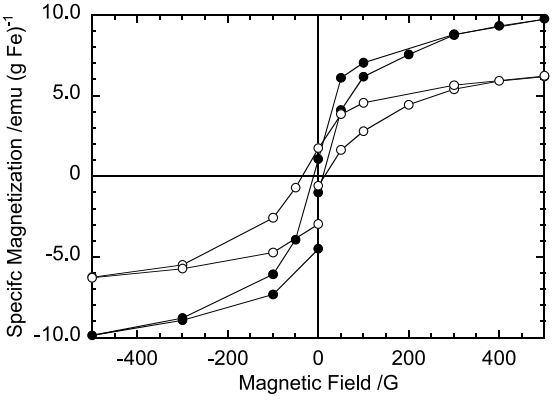

Fig. 2. Magnetization versus magnetic field plots for o-Fe-Alg(Sr) (●) and o-Fe-Alg(Ba) (○), measured at 300 K. The magnetization data presented are the specific ones normalized with the respective iron contents, as is also the case for Fig. 1.

Table 2
Summary of the estimation of magnetic properties for o-Fe-Alg/PVA samples at different temperatures

Sample code	Magnetism[a]				Specifc parameters at RT		
	20 K	100 K	200 K	RT[b]	M_s[c]/emu	H_c[d]/G	M_r[d]/emu
o-Fe-B1	–	–	–	DM	–	–	–
o-Fe-B2	Pseudo SPM	PM	PM	PM	–	–	–
o-Fe-B3	Pseudo SPM	Pseudo SPM	PM	PM	–	–	–
o-Fe-B4	Pseudo SPM	PM	PM	PM	–	–	–
o-Fe-B5	Pseudo SPM	Pseudo SPM	PM	PM	–	–	–
o-Fe-B6	FM	FM	SPM	SPM	2.92	–	–
o-Fe-B7	SPM	SPM	SPM	SPM	0.28	–	–
o-Fe-B8	SPM	SPM	SPM	SPM	0.48	–	–
o-Fe-B9	FM	FM	SPM	SPM	2.00	–	–
o-Fe-B10	FM	FM	SPM	SPM	1.36	–	–
o-Fe-B11	SPM	SPM	SPM	SPM	0.68	–	–
o-Fe-B12	SPM	SPM	SPM	SPM	0.77	–	–
o-Fe-Alg(Ca)	FM	FM	SPM	SPM	5.66	–	–
o-Fe-Alg(Sr)	–	–	–	FM	11.0	10.2	1.09
o-Fe-Alg(Ba)	–	–	–	FM	7.62	38.5	1.67

[a] DM, diamagnetic; PM, paramagnetic; SPM, superparamagnetic; FM, ferromagnetic.
[b] 298 K for samples o-Fe-B1 to B12, and 300 K for three o-Fe-Alg samples.
[c] Determined by a classical Langevin fitting to the specific magnetization data normalized with Fe content in a range 0–1000 G.
[d] Evaluated by a linear approximation to the specific magnetization data in a range +50 to −50 G.

in radius than Fe^{2+}, may be adaptable for the ideal in situ reaction attended by the ion-exchange. In the replacements with Sr^{2+} and Ba^{2+} of a considerably larger size, the reaction space for precipitating ferrous hydroxide could be spread to an appreciable degree. As a result, iron oxides synthesized in the following step would grow into comparatively larger particles, which may be responsible to the occurrence of M_r and H_c. However, there is still a possibility of another factor setting up the observation of the magnetic hysteresis; e.g., a sub-production of magnetic particles in such a form as $BaO \cdot 6Fe_2O_3$.

The superparamagnetic property of o-Fe-Alg(Ca) was maintained even after three cycles of the same reaction process. With the treble procedure, the saturation magnetization became more than 2 times that for the one cycle sample, following an increase in iron content to ca. 19 wt%; but the initial rise of the M versus H plot became rather gradual.

3.2. Iron oxide-containing Alg/PVA IPNs

The iron content evaluated for the o-Fe-Alg/PVA series, including samples coded as o-Fe-B1 to B12 in Table 1, was less than 12 wt% and, in general, higher at compositions of larger Alg proportions and in samples subjected to the alkali treatments (d) and (c) with $Ca(OH)_2$ for 24 h (see Experimental part). As summarized in Table 1, the samples o-Fe-B1 to B5 obtained via the treatment (a) with CaB_4O_7 only were not responsive to a bar magnet, while the others all responded more or less. It can be inferred that a sufficient number of iron oxides were not formed in the former samples. Particularly, when the polymer matrix was only PVA (o-Fe-B1), ferrous ions seemed hardly to permeate inside the borated gel to the naked eye. Concerning the borate agent $Na_2B_4O_7$ or CaB_4O_7 applied to the loosely crosslinking pre-treatment, the alternative choice appeared not to be a serious factor influencing the ferrous ion absorption in the following step. However, the direct steeping of the mixed polymer solutions in a bath of aqueous ferrous salt gave rise to partial dissolution of the PVA component out of the resulting gels.

Alginate gels containing iron oxides were usually fragile. In contrast, the blend networks with PVA were comparatively soft and durable, endowed with a deformability to compressive and extensional stresses. Fig. 3 shows three data of dynamic viscoelastic measurements; the storage modulus E' and loss modulus E'' are plotted as a function of vibration frequency for iron oxide-containing gels of Alg/PVA = 10/0, 7/3, and 5/5. The binary polymer gels correspond to the samples o-Fe-B10 and o-Fe-B12 in Table 1, and the o-Fe-Alg gel (not listed in Table 1) was prepared in a similar way via the alkali treatment (c). As can be seen from the data, the modulus E' of the alginate gel was approximately 2×10^5 Pa and the Alg/PVA gels assumed a smaller E' value situating around $5–6\times10^4$ Pa, when compared at frequencies of ≥ 1 Hz. The result of $E'' < E'$ in any case is in accordance with a general trend observed for never flowing polymer gels [21,22]. Also, the magnitude of $10^4–10^5$ order for E' may be reasonable, taking account of some modulus data available in literature, $\lesssim 10^4$ Pa for less crystalline PVA gels [21,23] and 2×10^6 Pa for a hard gel of agar [24].

The loss tan δ was assessed roughly as 0.1–0.2, 0.15–0.3, and 0.2–0.4 for the respective samples of Alg/PVA = 10/0, 7/3, and 5/5 in a frequency range of 1–10 Hz. The elevation of the loss factor with an increase in PVA content implies a

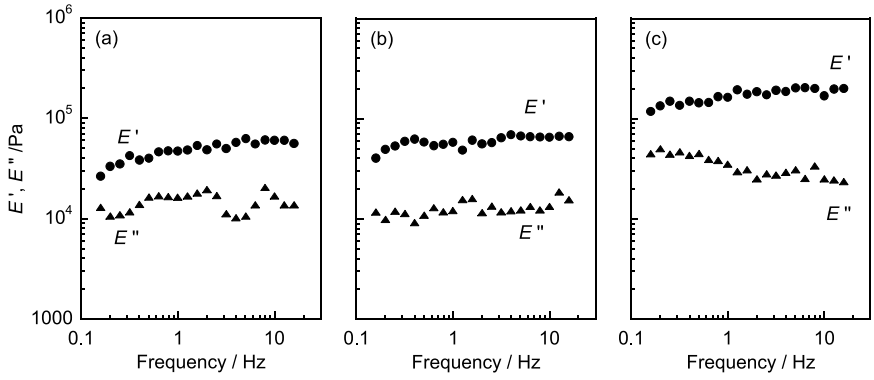

Fig. 3. Frequency dependence of the dynamic storage modulus E' and loss modulus E'' for iron oxide-containing Alg/PVA gels: (a) Alg/PVA = 5/5 (sample o-Fe-B12); (b) Alg/PVA = 7/3 (sample o-Fe-B10); (c) Alg/PVA = 10/0 (control sample).

shift from an elastic gel state to a relatively viscous one, supporting consistently the visual and tactile observations described above.

Magnetometry measurements were conducted for the binary polymer series at different temperatures, and the result is summarized briefly in Table 2, where the corresponding data for o-Fe-Algs are also included. First, their magnetization behaviour at room temperature is compared mutually, by exercising our caution to the difference in the Alg/PVA composition as well as to that in the alkali-treating method.

The PVA sample o-Fe-B1 was essentially diamagnetic (DM), reflecting the magnetism of the vinyl polymer. Four samples o-Fe-B2 to B5 were paramagnetic (PM), judged from a complete linear *M–H* relationship that is illustrated for o-Fe-B4 in Fig. 4. It can be reasonably assumed for these samples that magnetic iron oxides were not fully synthesized therein, but the PM nature of residual ferrous and/or ferric ions was superior to the DM ones of both polymer components. Seven samples o-Fe-B6 to B12, responsive to a permanent magnet, all exhibited a superparamagnetic (SPM) character at room temperature, as did the sample o-Fe-Alg(Ca). Fig. 4 demonstrates selected examples of the non-hysteretic *M* versus *H* plots. By application of Langevin

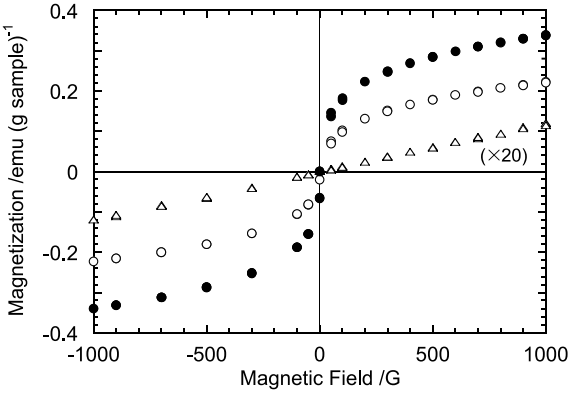

Fig. 4. Magnetization data obtained at 298 K for three o-Fe-Alg/PVA samples: (△), o-Fe-B4; (●), o-Fe-B6; (○), o-Fe-B9. The data for o-Fe-B4 are magnified by 20 times.

fitting to the respective specific magnetization data normalized with Fe content in a range 0–1000 G, M_s values for these samples of IPN series were estimated, which are also listed in Table 2.

In comparison of the M_s values of o-Fe-B7, B9, and B11 with those of o-Fe-B8, B10, and B12, respectively, no systematic correlation can be found between the sort of the borate crosslinker used and the saturating amplitude of magnetization. It can thus be presumed that the alternative for the pre-crosslinking did not influence the magnetic property of the iron oxide particles synthesized afterward within the respective gels. Then, comparing between o-Fe-B9 and B11, and between o-Fe-B10 and B12, each pair prepared by exactly the same chemical procedure, we find clearly a greater quantification of M_s for the Alg-richer composition. This is quite a natural result, since the polysaccharide component participates in the chelation with ferrous ions.

When a further comparison of M_s is made at a fixed polymer composition of 5/5, it results in a finding of the order of o-Fe-B6 ≫ B11 > B8 regarding the amplitude of the specific parameter. The same manner did hold with respect to their *M* values compared at an arbitrary *H*; but, all higher than the corresponding value for the paramagnetic sample o-Fe-B3. These observations indicate again an importance of the alkali-treating step for the in situ synthesis of magnetic iron oxide particles. In the employment of calcium tetraborate, the partial exchange of Fe^{2+} for Ca^{2+} should be possible in the junction zone of the Alg network; nevertheless, the liberated Fe^{2+} would rarely precipitate in the hydroxide structure, or rather diffuse out of the polymer matrix, without sufficient supply of hydroxyl ions. The use of $Ca(OH)_2$ ensures simultaneous attainment of the partial cation-exchange and the ensuing in situ precipitation of $Fe(OH)_2$ that is possibly indispensable as a precursor for the present magnetic ferrite synthesis. In view of controlling the size of the reaction cavity, however, the combined use of CaB_4O_7 and $Ca(OH)_2$ may be preferable, because it is capable of fastening the PVA network, too, by virtue of borate ions.

Finally, we discuss the temperature dependence of the magnetization behaviour of the o-Fe-Alg/PVA series. Table 2 lists the result of the estimation of apparent magnetism at temperatures lower than 300 K for the respective zero-field-cooled samples, the freezing being done without applying magnetic field before the isothermal *M–H* measurements. Fig. 5 exemplifies magnetization curves obtained at 20 and 100 K for o-Fe-B6 which exhibited a typical SPM regime at room temperature (see Fig. 4). The sample still retained this magnetic character at 200 K, whereas the magnetization curve at 20 K depicts a definite hysteresis loop, and even at 100 K there exist the remanence and coercivity of certain extents, as can be seen from the two corresponding data in Fig. 5. The observation suggests that a SPM to FM transition temperature is located just above 100 K. Such a transition in magnetism was also perceptible for the samples o-Fe-B9, B10, and o-Fe-Alg(Ca), which were prepared via the alkali treatment (d), or via the treatment (c) with an Alg-rich composition.

In contrast to the above, the samples o-Fe-B7, B8, B11, and B12, obtained via the treatment (b) or (c) with a composition of Alg/PVA = 5/5, gave no indication of magnetometric transition, all remaining a material of SPM nature at the low temperatures. Generally, the SPM to FM transition is correlated to a blocking phenomenon, in which the magnetic moments of the particles considered are frozen along their anisotropy axes. The critical temperature should shift depending on the distribution of the particle radius of gyration, lowered with a decrease in the average size of the particles. It is therefore conceivable for the four 5/5 IPN composites that the dimensions of the magnetic particles dispersed in were too minute to give rise to the transition in the temperature range investigated.

The samples o-Fe-B2 to B5 showed commonly a PM character at temperatures higher than 100 K. As the temperature was lowered to 20 K, however, the *M–H* plots deviated from the direct proportionality and indicated apparently SPM-like behaviour, but with a considerably low rate of curvature causing a less saturating action of the magnetization within the applicable range of H ($<5\times10^4$ G). Therefore the magnetic character is designated conventionally as pseudo SPM in Table 2.

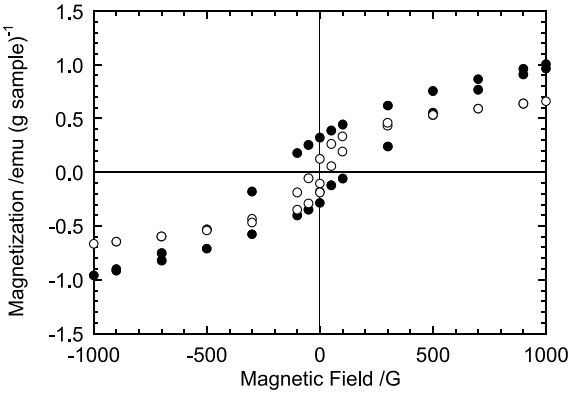

Fig. 5. Hysteretic magnetization curves observed for a sample o-Fe-B6 at 20 K (●) and 100 K (○).

4. Conclusions

Alginate/poly(vinyl alcohol) (Alg/PVA) composites with magnetic iron oxides were prepared successfully through adequate modification of the in situ synthesis technique [10] and, basically, by utilizing ion-associated chelation and gelation characteristics of both polymers. The magnetization versus magnetic field profiles were examined by SQUID magnetometry for the freeze-dried samples, and the dynamic mechanical property in their hydrogel state was also characterized.

The ferrous alginate sample oxidized in $Ca(OH)_2$ solution showed superpramagnetism, while the ones treated with $Sr(OH)_2$ and $Ba(OH)_2$ were of ferromagnetic character at room temperature. The result may be ascribed to the difference in the cation-exchanging manner affecting the dimension of the reaction space for ferrite synthesis in the polysaccharide network. The fragility of the gel matrix of alginate only was improved by the compatible blending with PVA and the simultaneous crosslinking of both components. As a result of this IPN construction, the composites became comparatively tenacious and deformative in the gelatinous state. The acquisition was made explicit by estimation of the viscoelasticity varying according to the Alg/PVA composition. In the binary polymer system, the magnetism was changeable depending on the alkaline treatment condition, polymer composition, and surrounding temperature, especially the first item regarding chemical processing being the key factor controlling the efficiency of the precipitation of $Fe(OH)_2$ as a precursor of magnetic iron oxide particles.

The observations of superparamagnetism (SPM) at room temperature for the majority of the IPN samples may be of significance for designing and diverse applications of new magnetic materials that are furnished with a mechanical processibility, in addition to the perceptibility to an external magnetic stimulus only on demand and with restraint of energy loss.

The topics of the present paper were restricted mainly to the preparation and magnetometric characterization of iron oxide-incorporated Alg/PVA networks. Further investigation should be required for estimation of the scale of the magnetic particles and their morphology, in correlation to the network structure. In a current experiment with a field emission scanning electron microscope, we have found fine metallic particles, measuring less than ~20 nm in diameter, to be dispersed within a composite sample exhibiting the SPM nature. More detailed characterization by microscopy and diffractometry for the present system is in progress, in parallel with a comparative study with other carbohydrate/synthetic polymer pairs.

Acknowledgements

The authors wish to acknowledge Dr A. Otsuka of Research Center for Low Temperature and Materials Sciences, Kyoto University, for his kind arrangement of the SQUID magnetometry measurements. This work was partially supported by a Grant-in-Aid for Scientific Research (B) (No. 14360201 to Y.N.) from Japan Society for the Promotion of Science.

References

[1] Marchessault RH, Ricard S, Rioux P. Carbohydr Res 1992;224:133.
[2] Marchessault RH, Rioux P, Raymond L. Polymer 1992;33:4024.
[3] Hamaya T, Takizawa T, Hidaka H, Horikoshi K. J Chem Eng Jpn 1993;26:223.
[4] Raymond L, Revol JF, Marchessault RH, Ryan DH. Polymer 1995;36:5035.
[5] Kroll E, Winnik FM, Ziolo RF. Chem Mater 1996;8:1594.
[6] Sourty E, Ryan DH, Marchessault RH. Cellulose 1998;5:5.
[7] Jones F, Cölfen H, Antonietti M. Colloid Polym Sci 2000;278:491.
[8] Llanes F, Ryan DH, Marchessault RH. Int J Biol Macromol 2000;27:35.
[9] Suber L, Foglia S, Ingo GM, Boukos N. Appl Organometal Chem 2001;15:414.
[10] Ziolo RF, Giannelis EP, Weinstein BA, O'Horo MP, Ganguly BN, Mehrotra V, Russell MW, Huffman DR. Science 1992;257:219.
[11] Fischer FG, Dörfel HZ. Physiol Chem 1955;302:186.
[12] Haug A, Larsen B, Smidsrød O. Acta Chem Scand 1966;20:183.
[13] Smidsrød O, Haug A. Acta Chem Scand 1972;26:2063.
[14] Grant GT, Morris ER, Rees DA, Smith PJC, Thom D. FEBS Lett 1973;32:195.
[15] Morris ER, Rees DA, Thom D, Boyd J. Carbohydr Res 1978;66:145.
[16] Clark AH, Ross-Murphy SB. Adv Polym Sci 1987;83:57.
[17] Draget KI, Smidsrød O, Skjåk-Bræk G. In: Vandamme EJ, De Baets S, Steinbüchel A, editors. Polysaccharides II. Polysaccharides from eukaryotes, biopolymers, Vol. 6. VCH Verlag: Wiley; 2002. p. 215–44.
[18] Miura K, Kimura N, Suzuki H, Miyashita Y, Nishio Y. Carbohydr Polym 1999;39:139.
[19] Grasdalen H, Larsen B, Smidsrød O. Carbohydr Res 1981;89:179.
[20] See, for example, (a) Zrínyi M. Trends Polym Sci 1997;5:280. (b) Moskowitz BM, Frankel RB, Walton SA, Dickson DPE, Wong KKW, Douglas T, Mann S. J Geophys Res 1997;102:22671.
[21] Te Nijenhuis K. Adv Polym Sci 1997;130:1.
[22] Hossain KS, Nemoto N, Nishinari K. Nihon Reoroji Gakkaishi 1997;25:135.
[23] He J, Horie K, Yokota R. Polymer 2000;41:4793.
[24] Horio M, Onogi S. J Appl Phys 1951;22:977.